Supplementary Information for

Nutrient-dependent growth underpinned the Ediacaran transition to large body size

Supplementary Methods

Measuring size growth

Rangeomorph body patterning is hypothesised to have followed a program of axial, sub-apical branching in which new lateral branches formed at the extremities of the frond 1 2. Once established, these branches continued to grow in size during life 1 2. However, the developmental mechanisms of size growth in fossil rangeomorphs have not previously been studied.

To infer patterns and rates of biological growth throughout ontogeny, we require measures of size (such as length, area and volume) and a way to estimate the change in size over time 3. For fossil organisms, the time component is usually unknown due to the coarse timescale of the geological record relative to biological lifespans. However the iterative branching of the rangeomorph frond 2 allows measurement of branch segment size against ordinal age in an iterative growth series (giving a scaling relationship which implicitly relates to time e.g. see 4). As a result, we can read back the sizes of sequential stem internodes to infer the history of internode growth.

To do this, 3D measurements were taken using micro-CT scans of an exceptionally preserved specimen of *Avalofractus abaculus* (Royal Ontario Museum specimen number 63005, replica of Rooms Museum specimen number NFM F-754, described in 5). This is a three-dimensional impression fossil (Fig. 1). The fossil was collected previously from bed FS-52 from the Trepassey Formation at Spaniard's Bay, Newfoundland (<565 Ma 6), which avoided significant compression, or deformation resulting from tectonic cleavage, and is

exceptionally fine-grained, consequently showing some of the best preservation known from the Ediacaran 5 6 7. The upper region of the fossil is moulded in positive relief and the lower in negative relief. These may represent exterior moulds of the upper and lower surfaces of the organism, although some interior body tissue may possibly have been cast 6 7, particularly in the central-lower, apparently decayed, region 6. The exposed central axis, or stem, can be polarised from youngest (apex) to oldest (base) independently of internode size. This orientation is based on the presence of an elongate basal stem segment (Fig. 1), which in other, complete specimens connects to an anchoring holdfast (8 Fig. 1.1), as well as a general increase in the length of the primary branches from the stem apex to base. Sequential stem internodes were identified as continuous unbranched segments between consecutive primary lateral branches (illustrated Fig. 1).

CT-data collection and analysis

3D micro-CT scanning of specimen ROM 63005 was performed using a Nikon Metrology XT H 225 high-resolution scanner at the Cambridge Biotomography Centre, using a voltage of 105 kV and current of 183 uA. The CT scan voxel resolution was 0.049 mm. A volume rendering was then reconstructed and virtually sliced, perpendicular to the specimen surface, at 0.33 mm intervals using the program Drishti 9. At each slice height, the cross-sectional width of the stem was measured, giving a total of 61 measurements at continuously distributed heights (Fig. 1, Fig. S1, Supplementary Table 1). There is a poorly preserved region, in which the stem is effaced, at the transition between comparatively well-preserved regions in positive versus negative relief (Fig. 1). Width values for cross-sections through this region of the fossil were excluded, leaving 46 stem width measurements (with 27 and 19, respectively, for the positive and negative relief regions, Supplementary Table 2).

Stem shape and retrodeformation

The cross-sectional stem shape was reconstructed, based on comparison of the measured width *w* and the perpendicular distance *b* from the midpoint to the surface of the stem (Fig. S1; Supplementary Table 2). Comparisons of cross-sectional width *w* and height *b* show that the stem is slightly vertically flattened (mean (*b*/*w*) was 0.34 with standard error SE = 0.035, n = 27 for the positive relief region and mean = 0.27, SE = 0.029, n = 19 for the negative relief region). Since the inferred axis of compression is approximately parallel to the direction of sedimentary compaction (vertical and perpendicular to the bedding surface), this can be attributed to slight post-mortem compression. An alternative possibility is that this is a biological feature, reducing internal volume relative to surface area. However, in practice, relative to the overall measurement range the effect on calculated volumes is very small (Fig. S2).

A retrodeformation calculation was performed to calculate the circular cross-sectional radius as $r = p/(2\pi)$ where p is the elliptical stem perimeter (calculated separately for the positive and negative relief regions). Elliptical stem perimeter was calculated as $p \approx 2\pi\sqrt{\frac{a^2+c^2}{2}}$ where $a = w/2$ and $c = w \times \text{mean}(b/w)$.

For stem segments, the lateral surface area ($SA_{lateral}$) and volume (V) were then calculated using the retrodeformed radius, treating each sampled stem segment as a circular conical frustum, where r_{apical} and r_{basal} are, respectively, the radii at the apical and basal ends, and l is the frustum length:

$$SA_{lateral} = \pi \times \left(r_{apical} + r_{basal}\right) \times \sqrt{\left(r_{apical} - r_{basal}\right)^2 + l^2} \quad (1)$$

$$V = \left(\frac{1}{3}\right) \times \pi \times l \times \left({r_{apical}}^2 + {r_{basal}}^2 + \left(r_{apical} \times r_{basal}\right)\right) \quad (2)$$

The distances from the stem apex at which the attachment between a lateral branch and the stem came into, and out of, view were also recorded, and the origination point of each lateral branch was measured as the mid-point between these distances (illustrated Fig. 1). The length of each stem internode was then calculated as the distance between adjacent primary lateral branch origination points (Supplementary Table 3).

Geometric calculations

A strong linear correlation between retrodeformed stem diameter and stem length (R^2 = 0.84, $p << 0.0001$) confirmed that the quality of fossil preservation in *Avalofractus abaculus* specimen ROM 63005 is sufficient to provide a consistent signal of biological scaling. Using Shapiro-Wilk tests, diameter values were confirmed to be normally distributed for both regions of the stem preserved in positive relief (n = 27, p = 0.77) and negative relief (n = 19, p = 0.39). To estimate the surface area (Eqn. 1) and volume (Eqn. 2) of sequential stem internodes (which are indicated in Fig. 1), the best-fitting relationship between stem length and diameter was first established in order to estimate the basal and apical diameter for each internode. To do this, curve fitting was used to test a range of standard biological growth curves 10 against observed size data, using MatLab and Curve Expert 2.3 (2011-2016 Daniel Hyams). Four alternative scaling functions of length (L) to diameter (D) for conical biological structures (following 10) were compared against retrodeformed stem measurements: half power, $L = D^{0.5}$, $D = L^2$; two-thirds power $L = D^{(2/3)}$, $D = L^{1.5}$; isometric (linear) $L = D^1$, $D = L^1$; and 1.5 power $L = D^{1.5}$, $D = L^{(2/3)}$ (Fig. S3). The best fitting scaling function was then selected based on the highest R^2 value, calculated from the residual differences between observed and predicted diameters ($R^2 = 1 - SS_{res}/SS_{tot}$ where SS_{tot} is the total sum of squared differences from the mean and SS_{res} is the sum of squared residuals). This indicated that isometric scaling of stem length to diameter (Fig. 1, Fig. S3) provides a better fit (R^2 = 0.37)

than either positive or negative allometric scaling (half power R^2 = 0.02, two-thirds power function R^2 = 0.27; 1.5 power function R^2 = 0.04). The surface area and volume of stem internodes were then calculated based on diameter values from the best fitting (isometric) scaling relationship (Fig. 1, Fig. S3).

3D growth models

For the null hypothesis of exponential internode growth, proportionate growth (the proportion, *r*, of current size by which internode size increases at the next growth step) remains constant throughout the growth period. For example, exponential growth is observed among populations of bacterial unicells with unlimited nutrient access 11, in the early growth of animal cancer tumours 12 and in young plants before limiting factors such as self-shading take effect 13. Under the null hypothesis of exponential growth, the volume (v) of a given rangeomorph branch internode which has gone through i growth steps is predicted to be:

$$v_i = v_0(1 + r)^i \tag{3}$$

Where v_0 is the starting volume of an internode, and *r* is the proportion of volume to be added at each growth step. Given iterative, apical lateral branching, which adds one new axial internode at each growth step, there will be $n + 1$ internodes at branch growth step n (with step numbering starting at zero). The total branch volume at step n is then given by the sum of sizes of all existing internodes:

$$Vn = \sum_{i=0}^{i=n} v_i \tag{4}$$

This is equivalent to:

$$Vn = v_0 \times \sum_{i=0}^{i=n} (1+r)^i$$

(5)

Which gives:

$$V_n = \left(v_0 \times \left((r+1)^{(n+1)} - 1\right)\right)/r$$

(6)

Under the alternative hypothesis of nutrient and size-dependent growth (Fig. 3b), total volume is also given by the sum of volumes of all existing internodes (Eqn. 4). However in this case, the proportionate growth in internode volume at a given growth step, denoted r_i, decreases between growth steps. Consequently, internode volume grows more slowly given size-dependent growth than under the null model of exponential growth. For size-dependent growth, the volume (v) of a given internode which has gone through i growth steps is:

$$v_i = v_0 + v_{i-1} \times r_{i-1} + v_{i-2} \times r_{i-2} +, \ldots, v_{i-i} \times r_{i-i}$$

(7)

Computer simulations

Growth in size of rangeomorph branch internodes was simulated, using MatLab scripts written by J.F.H.C. (Supplementary Computer Code), under alternative models of exponential volumetric growth (the null hypothesis), nutrient-dependent growth (the alternative hypothesis), and nutrient-dependent growth with varying nutrient levels (simulated vertically increasing nutrient gradient). The branching structure was specified using a simplified Lindenmayer-system (after 2), with two principal parameters: branching angle (specified at 45°) and internode volume (updated at each growth step according to the given growth model). For the exponential growth model, the volume (v_i) of a given internode was increased by the same proportion (r) at each step. The new length of the internode was then calculated by solving the equation relating volume of a conical frustum to length (l_i),

using the isometric scaling relationship of stem diameter (D) to stem length (L) based on measured data ($D = L \times 0.05$, Fig. 1):

$$v = \frac{1}{3} \times \text{pi} \times \left(l_{basal} - l_{apical}\right) \times \left({r_{apical}}^2 + \ (l_{basal} \times 0.025)^2 + \left(r_{apical} \times (l_{basal} \times 0.025)\right)\right) \quad (8)$$

Where l_{apical} is the length at the internode apex, l_{basal} is the length at the internode base, r_{apical} is the apical internode radius, and internode length is equal to $l_i = l_{basal} - l_{apical}$.

The nutrient-dependent growth simulations used a simple model in which the proportion of internode volume (r_i) to be added at a given growth step (i) was proportional to the relative surface area to volume ratio of the internode (SA/V), where r_0 is the starting proportion and SA_0/V_0 is the starting surface area to volume ratio:

$$r_i = r_0 \times \frac{SA_i/V_i}{SA_0/V_0}. \quad (9)$$

Environmental nutrient gradients were simulated by multiplying the size-dependent growth proportion (Eqn. 9) by a factor relating the internode's current position to the starting point (e.g. simulating linearly increasing nutrient levels with increasing vertical position, Fig. 3e).

1D growth models

CT-scan data from an exceptionally preserved specimen provides fine-scale, 3D information on the morphology and geometry of rangeomorph branches (Fig. 1). This is ideal since it allows the calculation and analysis of branch length, diameter, surface area and volume. However, most rangeomorph fossils do not expose the individual branches (including the stem) in 3D and the most common method for fossil digitisation has been photography. To facilitate analysis of photographic data, our 3D volumetric growth models can be projected down to give 1D predictions for growth in length. This enabled model

testing, using CurveExpert Professional version 2.5.3. Predicted growth curves were tested against measurements of the spacing, along the central axis, of primary lateral branches, from digital photographs of rangeomorph specimens. Where primary branches can be identified in a continuous alternating series, on well preserved specimens, the spaces between them indicate sequential stem internode lengths (e.g. Fig. 1). Additional specimens analysed in 1D were the holotype of *Charnia masoni* (replica held in the Department of Earth Sciences, University of Cambridge of Leicester City Museum specimen LEICT G279) and an undescribed South Australian Museum rangeomorph specimen, showing exceptional, fine-scale preservation.

The most important characteristic of exponential growth (the null hypothesis) is that size rises increasingly steeply, by the power of the growth step (Eqns. 3,6). Equation 6, describing cumulative exponential volume growth across stem internodes, is well represented by a simple exponential model: $y = ae^{bx}$ (Fig. S8) e.g. for curve fitting and model testing. Length can be expected to be proportionate to the cube root of volume: $v \sim l^3$ 14 and $l \sim \sqrt[3]{v}$ (precise equation for conical frusta Eqn. 2). Therefore, under the exponential volumetric model, length will also grow according to an exponential function (Fig. S9), though this curve will be less steep than that for volume (Fig. S8).

In contrast, nutrient-dependent growth that is affected by the surface area to volume ratio predicts that size will grow less steeply as growth proceeds (with size growing by a reduced proportion at each growth step). In the simulations conducted here, volumetric growth of an internode is proportionate to its surface area to volume ratio (Eqn. 9). Therefore, volumetric growth declines as internodes age, due their increasing size and decreasing surface area to volume ratio. Simulated nutrient-dependent growth in cumulative stem length, across sequential internodes, is well approximated by a simple quadratic function for curve fitting and model testing (Fig. S10).

Terminology

Throughout the manuscript, we use the term ‘nutrient’ to mean any substance required for metabolism and growth, including chemical elements such as oxygen (as is common in the biological literature 15) and compounds such as organic molecules. The term ‘tissue’ is also used in a general sense, meaning the composite cellular material of which an organism is composed, rather than implying any particular grade of organisation (e.g. with differentiated tissues).

Code availability

Computer code used in this study is provided in the online Supplementary Information.

Supplementary Figures

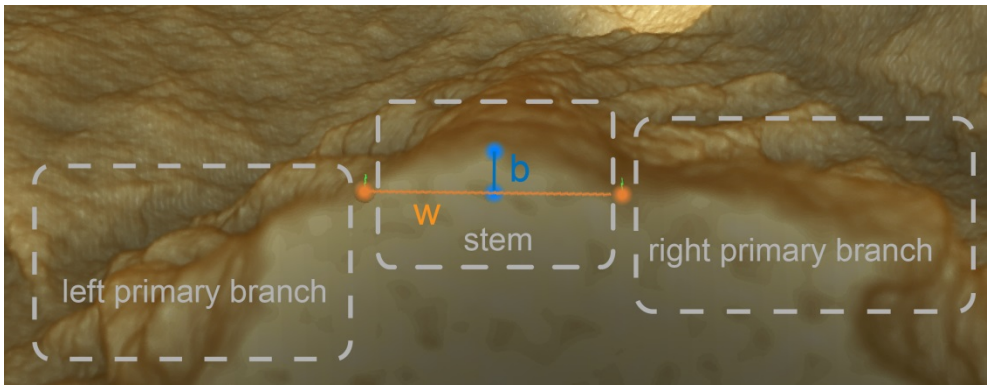

Figure S1. Virtual slice through a micro-CT scan of *Avalofractus abaculus* (specimen ROM 63005). This illustrates an example of cross-sectional stem width (*w*) and the perpendicular distance to the stem surface (*b*) for the positive relief stem region.

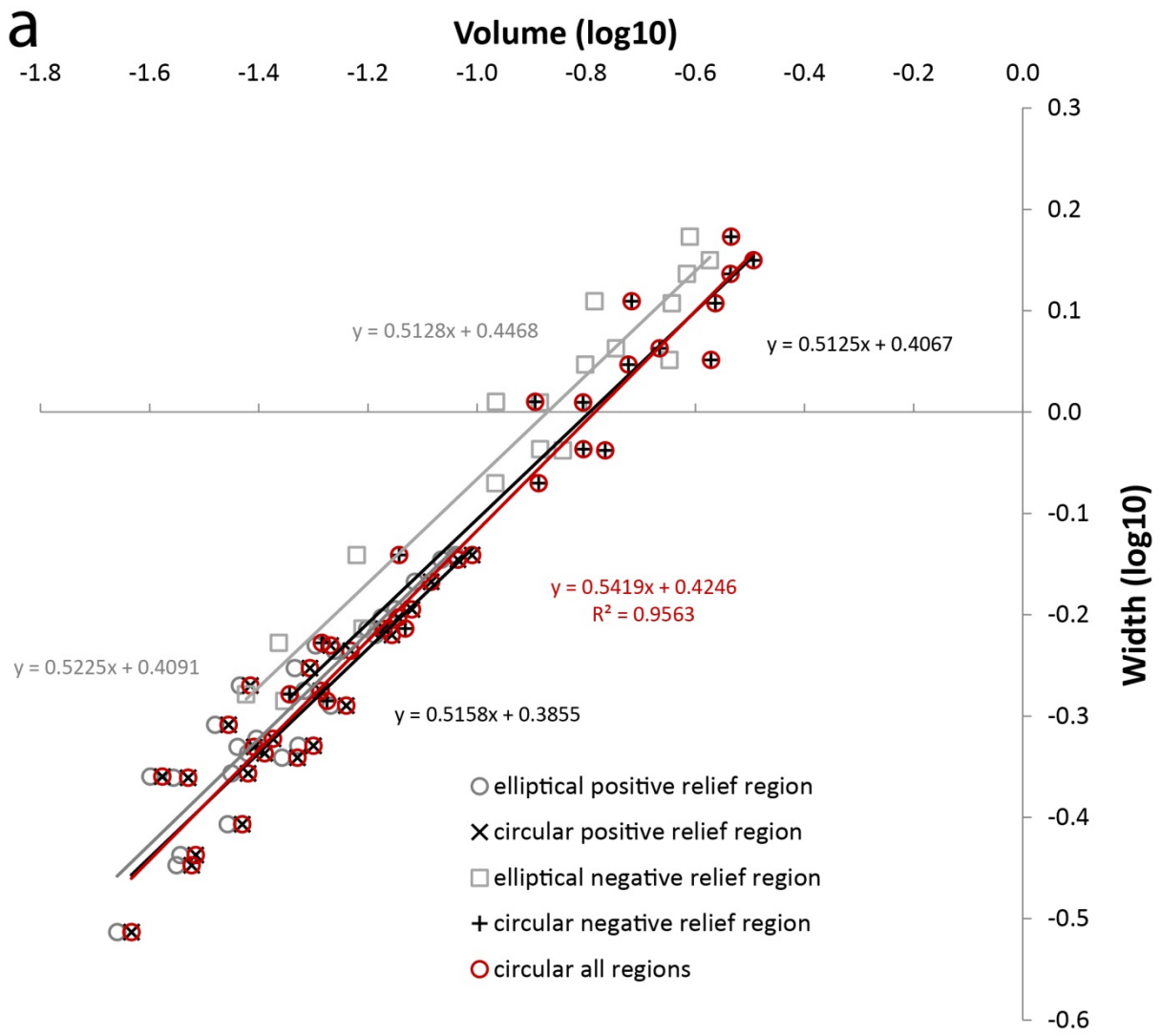
a
Volume (log10)
-1.8
-1.6
-1.4
-1.2
-1.0
-0.8
-0.6
-0.4
-0.2
0.0
0.3
0.2
0.1
0.0
-0.1
-0.2
-0.3
-0.4
-0.5
-0.6
Width (log10)
y = 0.5128x + 0.4468
y = 0.5125x + 0.4067
y = 0.5419x + 0.4246
R² = 0.9563
y = 0.5225x + 0.4091
y = 0.5158x + 0.3855
elliptical positive relief region
circular positive relief region
elliptical negative relief region
circular negative relief region
circular all regions

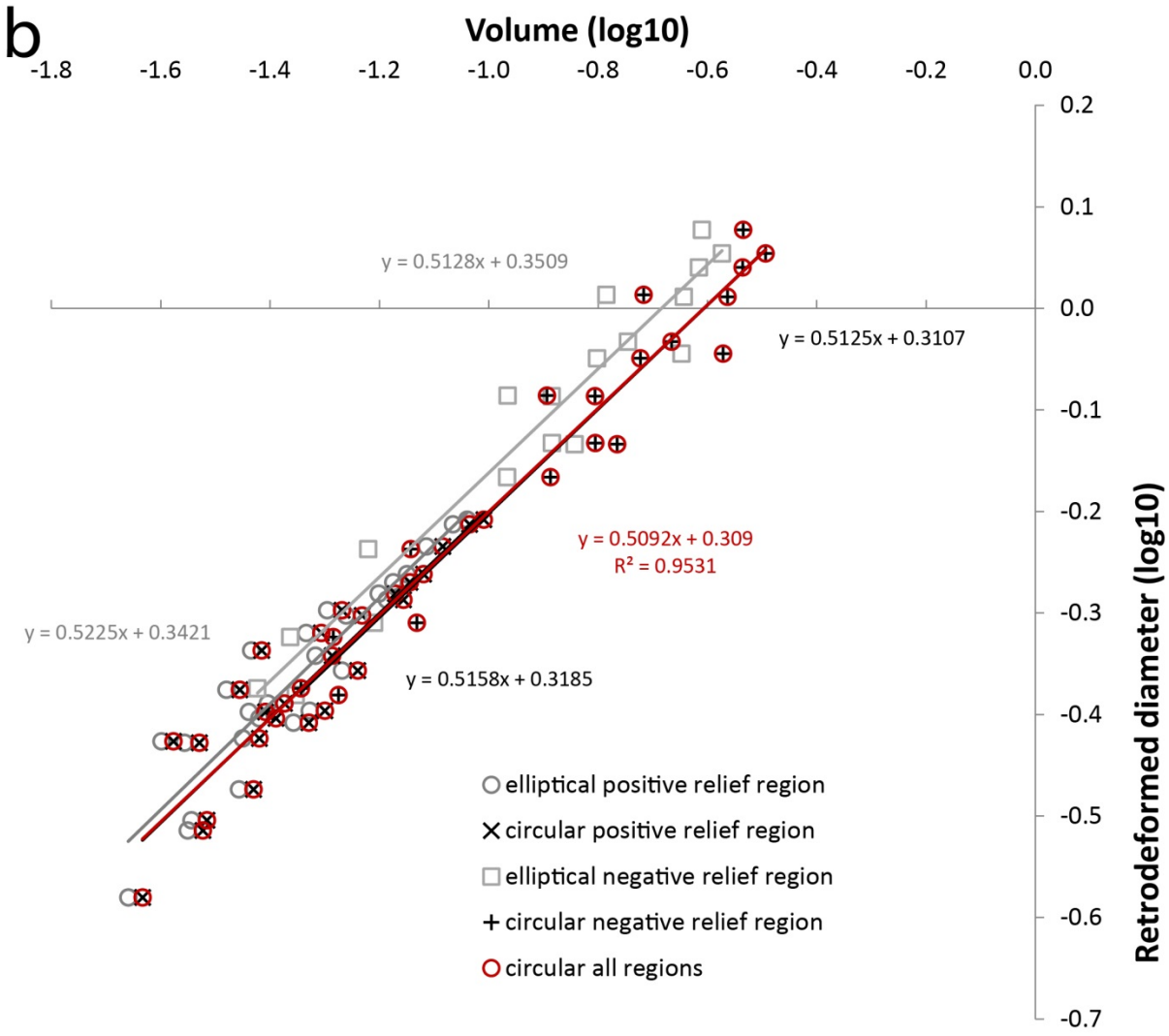

Figure S2. Calculated volumes for conical stem frusta. a, Calculated frustum volume plotted against measured frustum width (log 10). Calculated volumes for conical frusta treated as elliptical (with shape calculated from the measurement data as shown in Fig. S1) are only marginally lower than those calculated after retrodeformation to a circular cross-section. **b,** Calculated frustum volume plotted against retrodeformed frustum diameter (log 10). Linear regression lines are shown with their corresponding equations (matched colours).

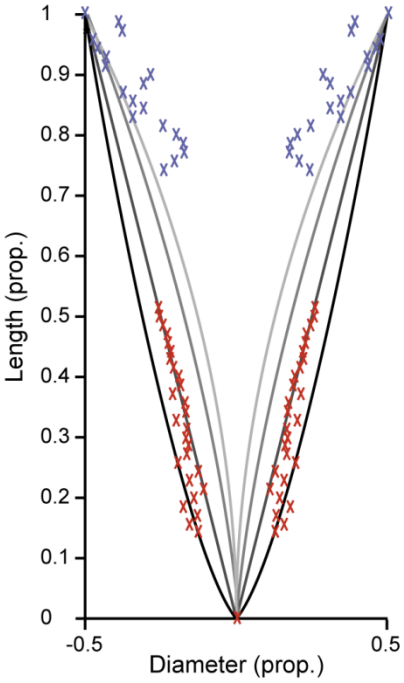

Figure S3. Retrodeformed stem diameter *D* for the positive relief stem region (red crosses) and negative relief stem region (blue crosses) versus length from the stem apex *L*. Values are shown as a proportion of the basal measurement. Diameter values were reflected and translated to the origin to illustrate stem diameter visually (with proportionate diameter indicated by the distance between the two data points at a given height), following 10. Lines show 4 alternative scaling models 10: half power, $L = D^{0.5}$, $D = L^{2}$ (light grey); two-thirds power $L = D^{(2/3)}$, $D = L^{1.5}$ (mid grey); isometric $L = D^{1}$, $D = L^{1}$ (dark grey); 1.5 power function $L = D^{1.5}$, $D = L^{(2/3)}$ (black). The isometric function (dark grey) is the best fit to the observed data (R^2 values: half power 0.02; two-thirds power 0.27; isometric 0.37; 1.5 power 0.04).

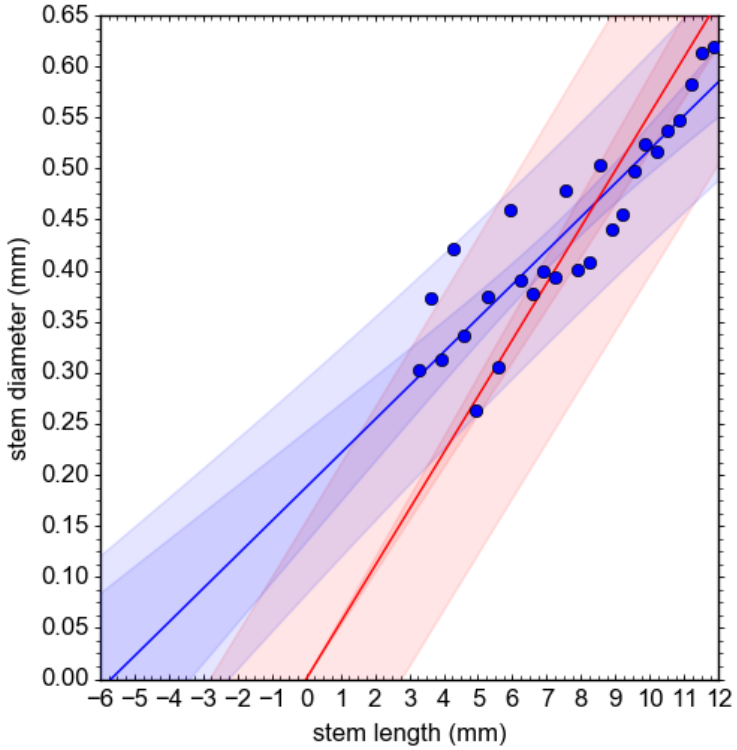

Figure S4. Retrodeformed stem diameter *D* for the positive relief stem region versus length from the stem apex *L* (blue circles). Blue line, linear regression with slope = 0.03, intercept = 0.19, R^2 = 0.80, $p < 0.0001$. Red line, linear regression with intercept constrained to zero, slope = 0.055, R^2 = 0.40, p = 0.0003. The 95% confidence band is shown in darker shading, the 95% prediction band is shown in lighter shading.

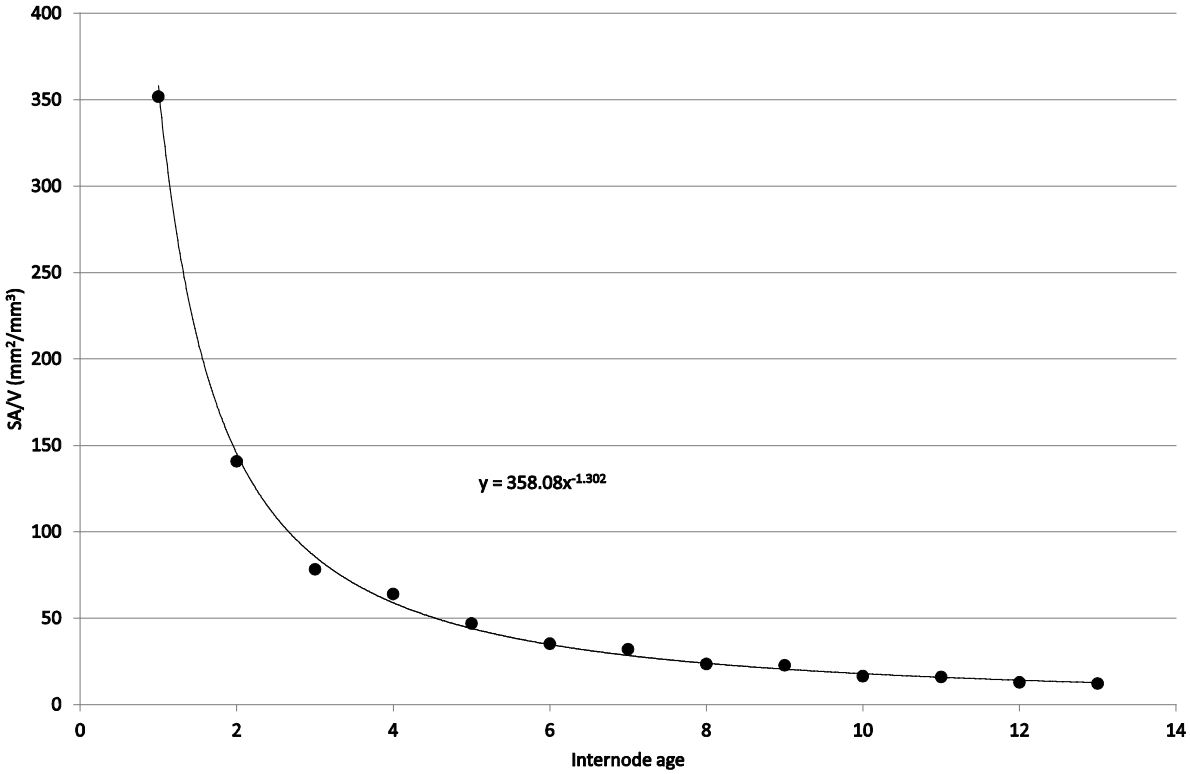

Figure S5. Stem surface area to volume ratio across internodes of increasing ordinal age. Cumulative surface area (SA) and volume (V) were calculated based on the inferred isometric scaling relationship for stem length and diameter (grey line on Fig. 1). The black line shows a power function fitted to these data. Inset text shows the equation for the function.

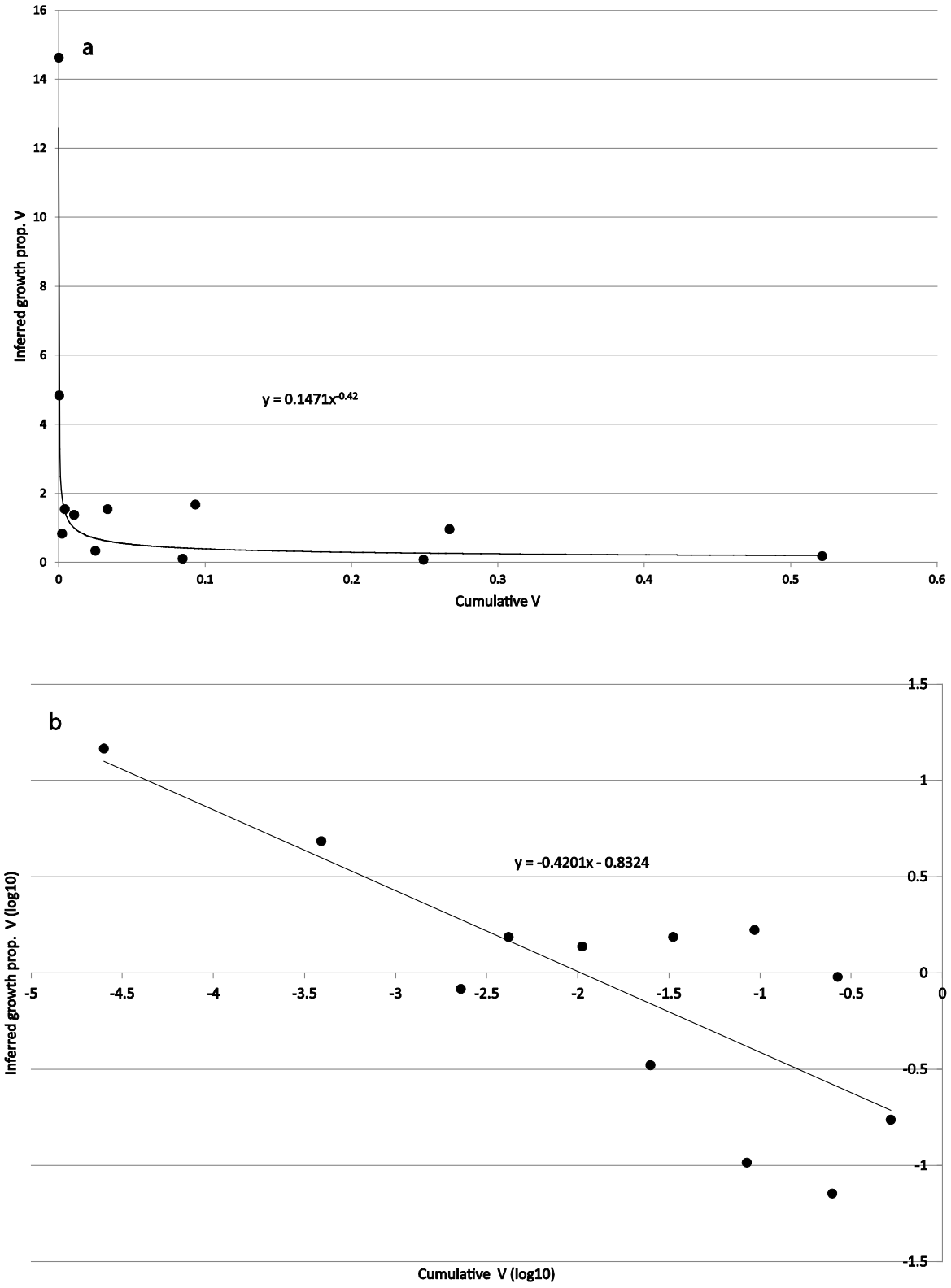

Figure S6. Inferred proportion of volume added along stem internodes of increasing ordinal age and volume. Cumulative volume (V) was calculated, treating internodes as conical frusta, based on the inferred isometric scaling relationship for length and diameter

(grey line on Fig. 1). Inset text shows the equation for a curve fitting the data. **a**, Untransformed data on a linear scale. The black line shows a power fit to the data. **b**, Log 10 transformed data (also shown in main text Fig. 2a). The black line shows a linear fit to the data, $R^2 = 0.64$, $p = 0.0019$ (compatible with a power function for untransformed data on a linear scale as shown in panel **a**).

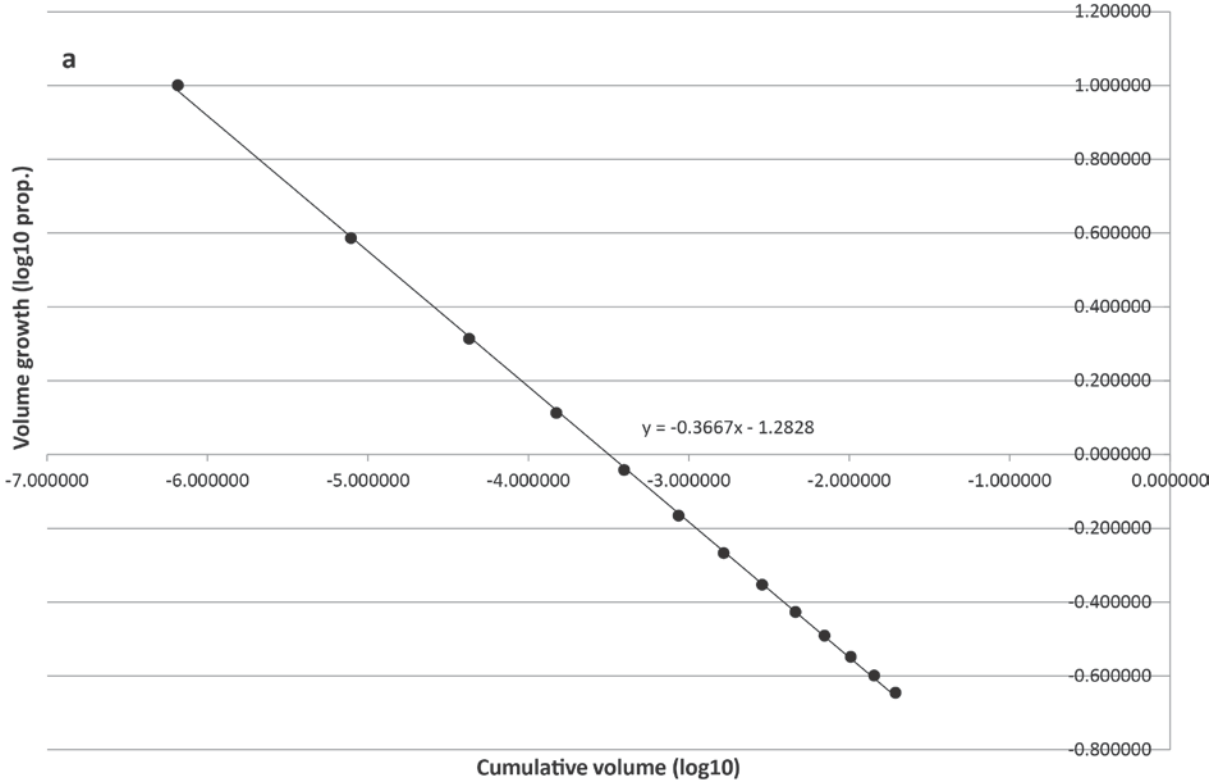

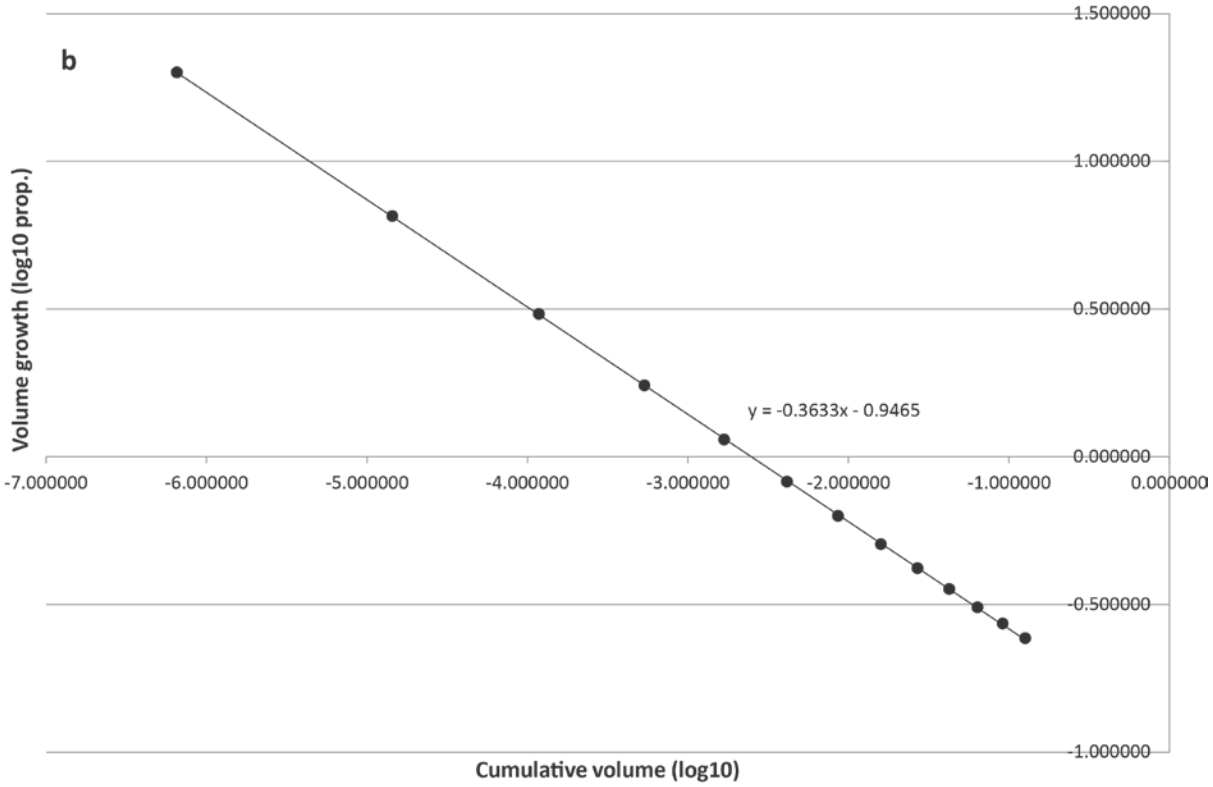

Figure S7. Proportion of volume added along stem internodes of increasing ordinal age and volume in computer simulations of nutrient-dependent growth. Computer simulations using the nutrient-dependent growth model predict a decline in proportionate internode volume growth at each growth step, similar to that observed for measured fossil data (Fig. S6b, above). In simulation, the precise slope of the decline depends on the starting growth proportion (figures show linear regression lines). E.g. with 13 growth steps and initial volume growth of 1000%, the slope is -0.3667 (**a**); with 2000% the slope is -0.3633 (**b**).

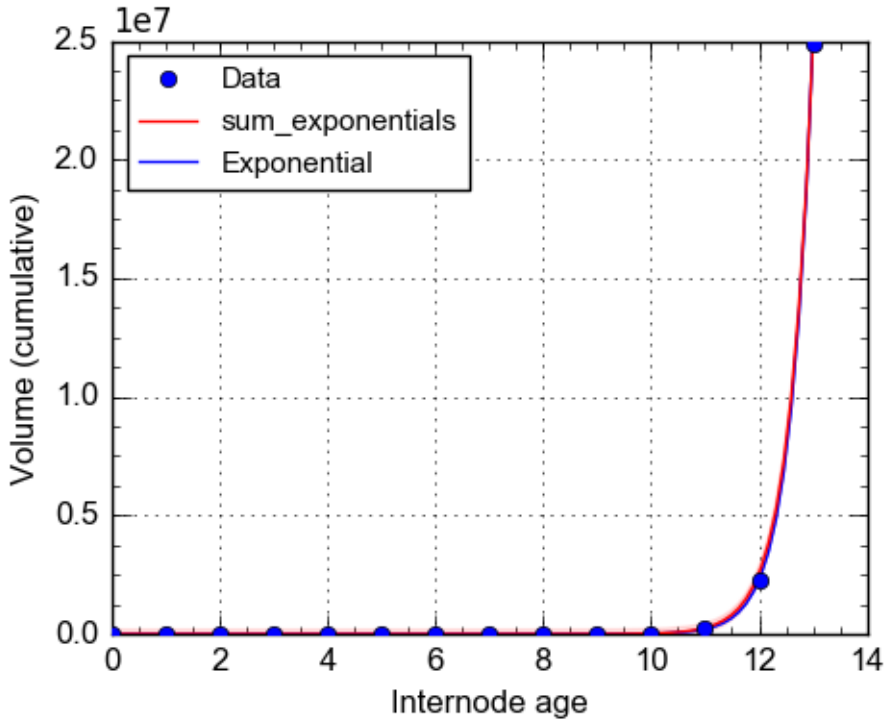

Figure S8. Curve fitting of an exponential curve to simulated exponential growth in cumulative stem volume. Simulated data for stem internodes (blue circles, arbitrary units) generated with a starting internode length of 0.1, volume of 6.54e-7, a proportionate volume increase of r = 10 at each step, over n = 13 growth steps. Both the summed exponential model (Eqn. 6) and simple exponential model ($y = ae^{bx}$, returning a = 0.038, b = 0.799) give an excellent, equal scoring (R^2 > 99%) fit to the simulated data (red line overlying blue line), confirming usefulness for model testing against real data.

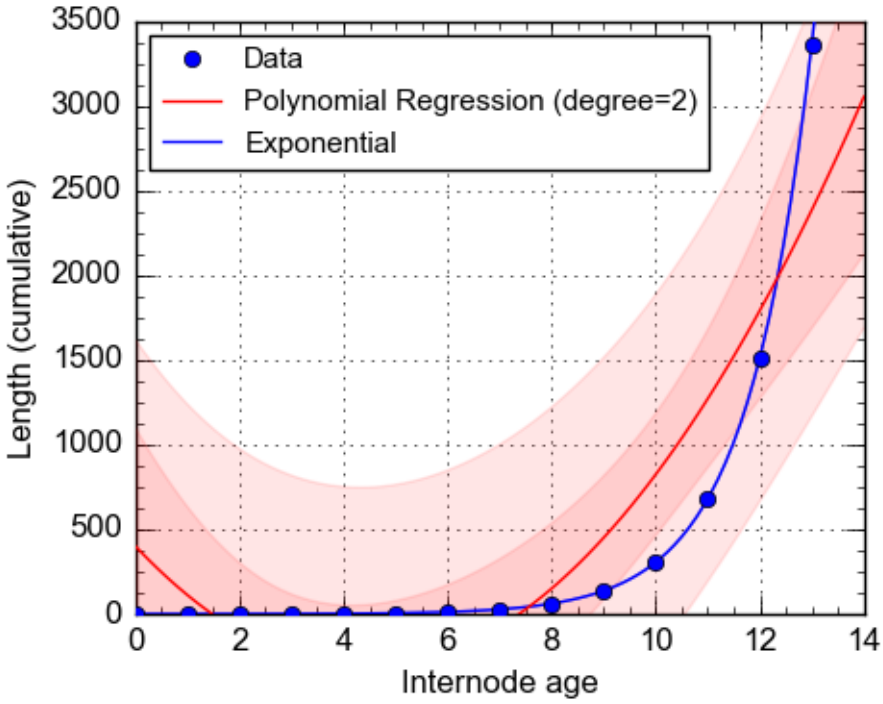

Figure S9. Curve fitting of an exponential curve to growth in cumulative stem length simulated under the exponential volumetric model. Simulation parameters: starting length = 0.1, starting volume = 6.54e-7, r = 10, n = 13. An exponential model, $y = ae^{bx}$, returning a = 0.10, b = 0.80, gives an excellent fit to the simulated data (R^2 > 99%), confirming its usefulness for model testing against real data. Under the *AIC* the exponential function (blue line) is confirmed to give a better fit, with likelihood 100%, than the quadratic function (red line), which is instead suitable for the nutrient-dependent growth model shown below in Fig. S10 (exponential *AICc* = -47.875, *dof* = 12, quadratic *AICc* = 173.007, *dof* = 11). 95% confidence band, darker shading; 95% prediction band, lighter shading.

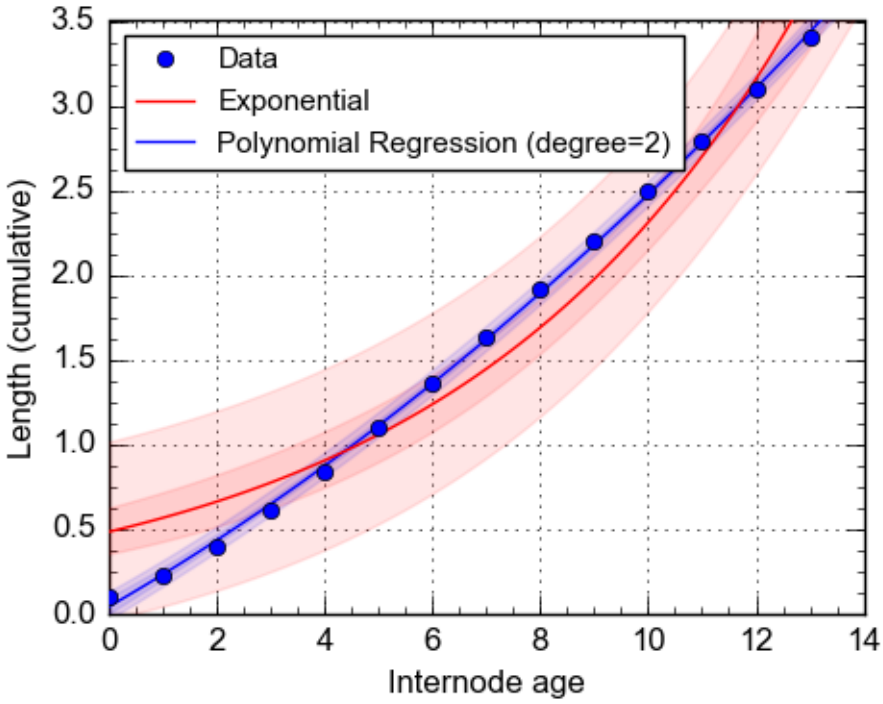

Figure S10. Curve fitting of a quadratic curve to growth in cumulative stem length simulated under the nutrient-dependent volumetric model. Simulation parameters: starting internode length 0.1, starting volume 6.54e-7, starting volume increase r = 10, n = 13 growth steps. A simple quadratic curve ($y = a + bx + cx^2$, returning a = 0.04, b = 0.18, c = 0.01) gives a good fit to the simulated data (R^2 > 99%), confirming its usefulness for model testing against real data. Under the *AIC* the quadratic function (blue line) is confirmed to give a better fit, with likelihood 100%, than the exponential function (red line), which is instead suitable for the exponential growth model shown in Fig. S9. *AICc* quadratic = -95.86, exponential = -40.63. 95% confidence band, darker shading; 95% prediction band, lighter shading.

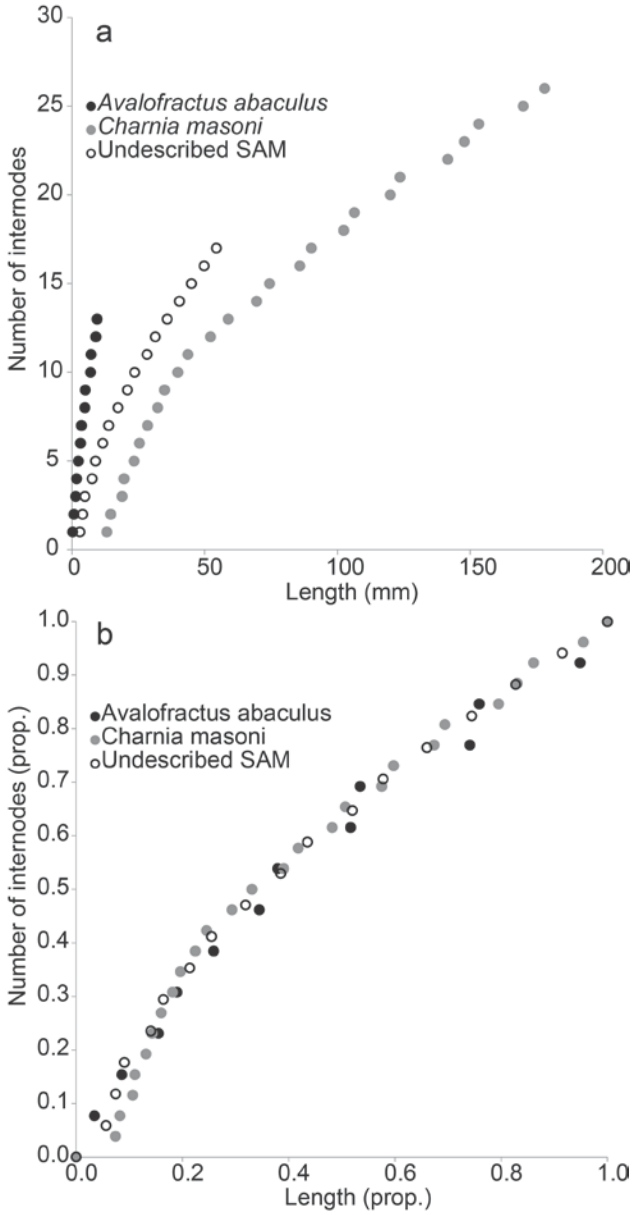

Figure S11. Number of stem internodes versus cumulative stem length among rangeomorph specimens. These data are also shown in Fig. 2. Here the axes are reversed for comparison to previous analyses of specimen total 'modules' (primary branches) versus length (e.g. 16). Comparative analyses of total specimen values consider the endpoints of individual growth trajectories **(a)**. Plotting data as the proportion of the maximum specimen value **(b)** illustrates that the patterns of growth are essentially indistinguishable after accounting for differences in total size. Specimens were *Avalofractus abaculus* ROM 63005

(black circles), *Charnia masoni* holotype replica (open circles) and an undescribed South Australian Museum specimen (grey circles).

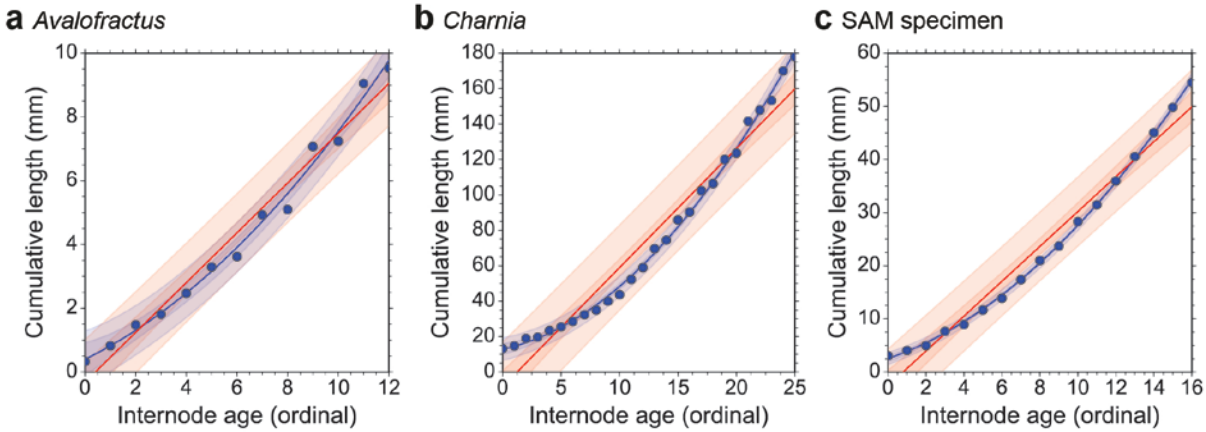

Figure S12. Curve fitting of linear and quadratic curves to growth in cumulative stem length. a, *Avalofractus abaculus* specimen ROM 63005. **b**, *Charnia masoni* holotype (replica). **c**, Undescribed South Australian Museum specimen. Fitted quadratic curves (blue lines), supporting nutrient-dependent growth (Fig. S10). Fitted null hypothesis (red lines) of linear growth. Akaike Information Criterion *AICc* (quadratic, linear) and corresponding likelihood that the quadratic curve is the better model: **a**, -27.69, -15.95, 99.7196%; **b**, 53.24, 126.72, 100%; **c**, -26.38, 37.00, 100%. Bands: 95% confidence (darker) and 95% prediction (lighter).

Supplementary References

1. Antcliffe, J. B. & Brasier, M. D., *Charnia* at 50: developmental models for Ediacaran fronds. *Palaeontology* **51**, 11-26 (2008).

2. Hoyal Cuthill, J. F. & Conway Morris, S., Fractal branching organizations of Ediacaran rangeomorph fronds reveal a lost Proterozoic body plan. *Proc. Natl. Acad. Sci. USA* **111** (36), 13122-13126 (2014).

3. Erickson, R. O., Modeling of plant growth. *Ann. Rev. Plant Physiol.* **27**, 407-434 (1976).

4. Klingenberg, C. P., Heterochrony and allometry: the analysis of evolutionary change in ontogeny. *Biol. Rev.* **73**, 79-123 (1998).

5. Narbonne, G. M., Laflamme, M., Greentree, C. & Trusler, P., Reconstructing a lost world: Ediacaran rangeomorphs from Spaniard's Bay, Newfoundland. *J. Paleont.* **83**, 503-523 (2009).

6. Narbonne, G. M., Modular construction of early Ediacaran complex life forms. *Science* **305**, 1141-1144 (2004).

7. Brasier, M. D. *et al.*, Explaining the exceptional preservation of Edicaran rangeomorphs from Spaniard's Bay, Newfoundland: a hydraulic model. *Precambrian Res.* **231**, 122-135 (2013).

8. Laflamme, M., Modeling morphological diversity in the oldest large multicellualr organisms. *PNAS* **111**, 12962-12963 (2014).

9. Limaye, A., *Drishti - Volume exploration and presentation tool*, presented at Vis, 2006, Baltimore, 2006 (unpublished).

10. Niklas, K. J., Size-dependent allometry of tree height, diameter and trunk-taper. *Ann. Bot.* **75**, 217-227 (1995).

11. Iyer-Biswas, S. *et al.*, Scaling laws governing stochastic growth and division of single bacterial cells. *Proc. Natl. Acad. Sci. USA* **111**, 15912-15917 (2014).

12. Benzekry, S. *et al.*, Classical mathematical models for description and prediction of experimental tumor growth. *PLoS Comput. Biol.* **10**, e1003800 (2014).

13. Paine, C. E. & et al, How to fit nonlinear plant growth models and calculate growth rates: an update for ecologists. *Methods in Ecology and Evolution* **3**, 245-256 (2012).

14. Okie, J. G., General models for the spectra of surface area scaling strategies of cells and organisms. *The American Naturalist* **181**, 421-439 (2013).

15. Garcia Camacho, F. *et al.*, A bioreaction-diffusion model for growth of marine sponge explants in bioreactors. *Appl. Microbiol. Biotechnol.* **73**, 525-532 (2006).

16. Gehling, J. G. & Narbonne, G. M., Spindle-shaped Ediacara fossils from the Mistaken Point assemblage, Avalon Zone, Newfoundland. *Can. J. Earth. Sci.* **44**, 367-387 (2007).